



Axisymmetric yielding of functionally graded spherical vessel under thermo-mechanical loading

Mojtaba Sadeghian*, Hamid Ekhteraei Toussi

Faculty of Engineering, Ferdowsi University of Mashhad, Mashhad 9177948944, Islamic Republic of Iran

ARTICLE INFO

Article history:

Received 14 September 2010
Received in revised form 25 October 2010
Accepted 27 October 2010
Available online 19 November 2010

Keywords:

Functionally Graded Material
Thermal stress analysis
Elastic perfectly plastic material
Elastic–plastic analysis
Yielded region borderline

ABSTRACT

Primarily the separate distributions of elastic and perfectly plastic thermal stress in spherical pressure vessels made up of Functionally Graded Material (FGM) are represented. Next, the combined elastic and perfectly plastic thermal stress analysis of a spherical pressure vessel is considered. It is assumed that no unloading is occurred and the modulus of elasticity, yielding stress and some specific material characteristic parameters are power functions of radius. In a spherical FGM vessel and for different material compositions, the effect of pressure and temperature upon the growth of plastic zone is studied. Especially the change in the position of the borderline between the elastic and plastic regions is sought. In an extensive range of material thermo-mechanical properties, the position of the elastic–plastic interface line and the yield pattern, which shows the number of plasticized layers in the wall of the vessel, are indicated.

© 2010 Elsevier B.V. All rights reserved.

1. Introduction

In this paper, the problem of thick-walled Functionally Graded (FG) spherical vessel under internal pressure and heat flux is studied. Although the analysis of thick walled spherical pressure vessels is a well-known subject in the literature, the analysis of inhomogeneous pressure vessels is not such a customary study. Nowadays due to the growing demand for the application of the Functionally Graded Materials in the construction of engineering structures, the need for the analytical solutions of these problems is gaining momentum. A summary of the recent research work as shown below, confirms this notion.

Some of the leading papers in the stress analysis of FG pressure vessels are those that study the effect of internal pressure on the distribution of stress in the vessel. Among these studies, one can point to the works by Horgan and Chan [1], Tutuncu and Ozturk [2]. The other groups of research works study the effect of thermal loads on the stress distribution in the elastic FG pressure vessels. The work of Zhang et al. [3], Takezono et al. [4], Wetherhold et al. [5], Zimmerman and Lutz [6], Obata et al. [7], Awaji and Sivakumar [8] belong to this category. The papers cover a wide range of geometries and thermal boundary conditions. There are also establishing works that discuss the mutual effect of thermal and mechanical loads on the FG structures. The papers of Reddy and Chin [9], Mequid and Woo [10], Jabbari et al. [11], Poultangari

et al. [12], Liew et al. [13], Eslami et al. [14], Araslan and Akis [15], Eslami and Bahtui [16], Akis [17] are some leading works in this category. Yet, for the analysis of FG structures, some other disciplinarians are adopted by researchers. For example, the size optimization can be seen in the works of Obota and Noda [18], Ootao et al. [19] and the stability analysis can be traced back in the works of Shen [20] and Shahsiah and Eslami [21].

The similarity between the abovementioned works in the stress analysis of FG structures is that all of them belong to the category of elastic media stress analysis. A different and yet more recent approach is to run into the study of plastic deformation. The works of Alshits and Kirchner [22] and Oral and Anlas [23] belong to this category.

Although there are special research reports that depict the simultaneous influence of thermal and mechanical loads on the elastic pressure vessels, so far no thermal–elastic–plastic analysis of FGM spherical vessels is reported. Therefore, in this study, the thermal stress analysis for a spherical pressure vessel made of inhomogeneous and Elastic–Perfectly Plastic (EPP) material is provided. The vessel is a thick walled FGM sphere with inner radius (a) and outer radius (b). It is under axi-symmetric steady state temperature and internal pressure distribution. It is also assumed that the outer surface is in zero pressure and temperature conditions. Mechanical and thermal properties along the radius are distributed according to a power law function. The problem is modeled by considering its Navier governing equation in both elastic and plastic regimes along with the Fourier heat conduction equation. The results are presented in the form of several case studies and charts.

* Corresponding author. Tel.: +98 915 5130325; fax: +98 511 8763304.
E-mail address: mo_sa257@stu-mail.um.ac.ir (M. Sadeghian).

Nomenclature

<i>a</i>	inner radius	<i>p</i>	plastic region indicator
<i>b</i>	outer radius	<i>q</i>	a material parameter
<i>C</i> ₁₁ , <i>C</i> ₂₁	convection thermal coefficients	<i>r</i>	radius
<i>C</i> ₂₁ , <i>C</i> ₂₂	conduction thermal coefficients	<i>T</i>	total strain indicator
<i>E</i>	Young's modulus of elasticity	<i>T</i>	temperature
<i>E</i> ₀	a material parameter	<i>Y</i>	yield stress
<i>e</i>	elastic region indicator	<i>Y</i> ₀	a material parameter
<i>K</i>	thermal conductivity	<i>α</i>	thermal expansion coefficient
<i>K</i> ₀	a material parameter	<i>α</i> ₀	a material parameter
<i>m, n, L</i>	some material parameters	<i>ν</i>	Poisson's ratio
<i>P</i> _a	internal pressure	<i>ε</i>	strain
<i>P</i> _b	external pressure	<i>σ</i>	stress

2. FG vessel thermal stress analysis

In this analysis, the problem of axi-symmetric and small deformation distribution of thermal stress and plasticity in an Elastic-Perfectly Plastic (EPP) spherical pressure vessel made of inhomogeneous Functionally Graded Material (FGM) is considered. Fig. 1 shows a typical FGM spherical vessel. In the spherical coordinates (*r, θ, φ*) the characteristic parameters of the vessel are assumed to be some power functions of *r*. It means that [12,17],

$$E(r) = E_0 r^n \tag{1}$$

$$Y(r) = Y_0 r^m \tag{2}$$

$$\alpha(r) = \alpha_0 r^L \tag{3}$$

$$K(r) = K_0 r^q \tag{4}$$

where $E_0 = \bar{E}/b^n$, $Y_0 = \bar{Y}/b^m$, $\alpha_0 = \bar{\alpha}/b^L$, $K_0 = \bar{K}/b^q$, \bar{E} , \bar{Y} , $\bar{\alpha}$ and \bar{K} are the referential parameters for the elastic modulus, yield stress, thermal expansion coefficient, and thermal conductivity respectively. Moreover *b* is the outer radius of the spherical vessel and *m, n, L*, and *q* as well as the Poisson's ratio (*ν*) are the parameters which do not depend on temperature.

For a spherical vessel in an infinitesimal and axi-symmetric deformation pattern the general constitutive relation is,

$$\epsilon_r^T(r) = \frac{1}{E(r)} [\sigma_r(r) - 2\nu\sigma_\theta(r)] + \epsilon_r^p(r) + \alpha(r) \cdot T(r) \tag{5}$$

$$\epsilon_\theta^T(r) \langle = \epsilon_\theta^T(r) \rangle = \frac{1}{E(r)} [(1 - \nu)\sigma_\theta(r) - \nu\sigma_r(r)] + \epsilon_\theta^p(r) + \alpha(r) \cdot T(r) \tag{6}$$

in which ϵ stands for strain and σ is stress. The superscript T means "total", while the superscript *p* is the sign of plasticity, $E(r)$ is elastic modulus function, $\alpha(r)$ is thermal expansion coefficient and $T(r)$ is the radial distribution of temperature in a vessel.

The strain and deformation components are related by,

$$\epsilon_r^T(r) = \frac{du(r)}{dr} \tag{7}$$

$$\epsilon_\theta^T(r) = \frac{u(r)}{r} \tag{8}$$

in which $u(r)$ is the radial displacement function.

2.1. Elastic analysis

In this section an elastic thermal stress analysis for a FG spherical vessel is given. Using Eqs. (5)–(8) the stress components are,

$$\sigma_r(r) = \frac{E(r)}{(1 + \nu)(1 - 2\nu)} \left[(1 - \nu) \frac{du(r)}{dr} + 2\nu \frac{u(r)}{r} - (1 + \nu)\alpha(r)T(r) \right] \tag{9}$$

$$\sigma_\theta(r) = \frac{E(r)}{(1 + \nu)(1 - 2\nu)} \left[\nu \frac{du(r)}{dr} + \frac{u(r)}{r} - (1 + \nu)\alpha(r)T(r) \right] \tag{10}$$

The equilibrium equation for a spherical vessel in an axi-symmetric problem is,

$$\frac{d\sigma_r}{dr} + \frac{2(\sigma_r - \sigma_\theta)}{r} = 0 \tag{11}$$

The substitution of Eqs. (9) and (10) in Eq. (11) results in the Navier equation of the problem as,

$$\frac{d^2u(r)}{dr^2} + \left[\frac{n+2}{r} \right] \frac{du(r)}{dr} + \left[\frac{2\nu(n+1)-2}{r^2(1-\nu)} \right] u(r) = \frac{(1+\nu)\alpha_0 r^L}{(1-\nu)} \left[\frac{n+L}{r} T(r) + \frac{dT(r)}{dr} \right] \tag{12}$$

One dimensional spherical steady state thermal conduction equation is [14],

$$\frac{1}{r^2} (r^2 K(r) T'(r))' = 0 \tag{13}$$

FGM hollow spherical vessel thermal boundary conditions are,

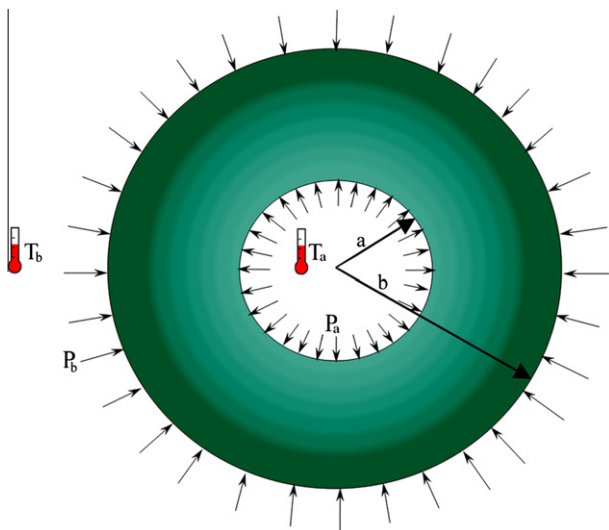


Fig. 1. Inhomogeneous spherical pressure vessel.

$$C_{11}T'(a) + C_{12}T(a) = f_1 \tag{14}$$

$$C_{21}T'(b) + C_{22}T(b) = f_2 \tag{15}$$

in which C_{11} and C_{21} are convection thermal coefficients, C_{21} and C_{22} are conduction thermal coefficients, f_1 and f_2 are specific constants in the inner and outer radius and a is the internal radius. Substituting thermal conductivity from Eq. (4) into Eq. (13) one obtains,

$$\frac{1}{r^2} (r^{q+2}T'(r))' = 0 \tag{16}$$

Solving Eq. (16), the distribution of temperature is found. Using temperature boundary conditions, one obtains,

$$T(r) = C_1 r^{-(q+1)} + C_2 \tag{17}$$

$$C_1 = \frac{C_{22}f_1 - C_{12}f_2}{C_{12}((q+1)C_{21}b^{-(q+2)} - C_{22}b^{-(q+1)}) - C_{22}((q+1)C_{11}a^{-(q+2)} - C_{12}a^{-(q+1)})} \tag{18}$$

$$C_2 = \frac{f_1((q+1)C_{21}b^{-(q+2)} - C_{22}b^{-(q+1)}) - f_2((q+1)C_{11}a^{-(q+2)} - C_{12}a^{-(q+1)})}{C_{12}((q+1)C_{21}b^{-(q+2)} - C_{22}b^{-(q+1)}) - C_{22}((q+1)C_{11}a^{-(q+2)} - C_{12}a^{-(q+1)})} \tag{19}$$

To solve the Navier equation in an uncoupled thermo-mechanical problem, primarily the distribution of temperature must be calculated. A general solution of Eq. (12) is the sum of the general solution of its relevant homogeneous form combined with the particular solution of the completely unbroken equation. The general solution of the homogeneous part is,

$$u_g(r) = Ar^s \tag{20}$$

Substituting Eq. (20) in homogeneous form of Eq. (12) one obtains,

$$u_g(r) = A_1 r^{S_1} + A_2 r^{S_2} \tag{21}$$

$$S_{1,2} = \frac{-(n+1) \pm \sqrt{n^2 + \frac{2n(1-5\nu)+9(1-\nu)}{1-\nu}}}{2} \tag{22}$$

A_1 and A_2 are some constants depended on the boundary conditions.

A particular solution of Navier equation is,

$$u_p(r) = E_1 r^{L+1} + E_2 r^{L-q} \tag{23}$$

Substituting Eq. (23) in Eq. (12) one obtains,

$$E_1 = \frac{(1+\nu)\alpha_o(n+L)C_2}{(1-\nu)[L^2 + (3+n)L] + n(1+\nu)} \tag{24}$$

$$E_2 = \frac{(1+\nu)\alpha_o(n+L-q-1)C_1}{(1-\nu)[(L+q)^2 + (1+n)(L-q-2)] - 2} \tag{25}$$

Now the general solution of Eq. (12) is,

$$u_T(r) = u_g(r) + u_p(r) = (A_1 r^{S_1} + A_2 r^{S_2}) + (E_1 r^{L+1} + E_2 r^{L-q}) \tag{26}$$

Taking P_a as the internal and P_b as the external pressure and substituting Eq. (26) into Eq. (9) the radial stress in terms of radial displacement is obtained as,

$$\sigma_r(r) = \frac{-E_o}{(1+\nu)(1-2\nu)} [A_1 r^{n+S_1} ((\nu-1)S_1 - 2\nu) + A_2 r^{n+S_2} ((\nu-1)S_2 - 2\nu) + r^{L+n+1} \{E_1(L(\nu-1) - (\nu+1)) + C_2\alpha_o(1+\nu)\} + r^{L+n-q} \{E_2((L-q)(\nu-1) - 2\nu) + C_1\alpha_o(1+\nu)\}]. \tag{27}$$

Moreover, using the boundary conditions of the problem, the constants A_1 and A_2 are obtained as,

$$A_1 = \frac{\varphi(b, S_2)[P_a - \zeta(a)] - \varphi(a, S_2)[P_b - \zeta(b)]}{\varphi(a, S_1)\varphi(b, S_2) - \varphi(a, S_2)\varphi(b, S_1)} \tag{28}$$

$$A_2 = \frac{\varphi(a, S_1)[P_a - \zeta(a)] - \varphi(a, S_2)[P_b - \zeta(b)]}{\varphi(a, S_1)\varphi(b, S_2) - \varphi(a, S_2)\varphi(b, S_1)} \tag{29}$$

in which,

$$\varphi(r, s) = \frac{E_o}{(1+\nu)(2\nu-1)} [(v-1)S - 2\nu] r^{m+s} \tag{30}$$

$$\zeta(r) = \frac{E_o}{(1+\nu)(2\nu-1)} [(C_2\alpha_o(1+\nu) + E_1(L(\nu-1) - (\nu+1)))r^{q+1} + (C_1\alpha_o(1+\nu) + E_2((L-q)(\nu-1) - 2\nu))]r^{n+L-q} \tag{31}$$

$$\tag{17}$$

$$\tag{18}$$

$$\tag{19}$$

Tangential stresses and radial-tangential strains in elastic regime can be found to be,

$$\sigma_\theta(r) = \frac{E_o}{(1+\nu)(1-2\nu)} [A_1 r^{n+S_1} (\nu S_1 + 1) + A_2 r^{n+S_2} (\nu S_2 + 1) + r^{L+n+1} \{E_1(1+\nu(L+1)) - C_2\alpha_o(1+\nu)\} + r^{L+n-q} \{E_2((L-q)\nu + 1) - C_1\alpha_o(1+\nu)\}] \tag{32}$$

$$\varepsilon_r(r) = A_1 S_1 r^{S_1-1} + A_2 S_2 r^{S_2-1} + E_1(L+1)r^L + E_2(L-q)r^{L-q-1} \tag{33}$$

$$\varepsilon_\theta(r) = A_1 r^{S_1-1} + A_2 r^{S_2-1} + E_1 r^L + E_2 r^{L-q-1} \tag{34}$$

2.2. Perfectly plastic analysis

In this section according to the Tresca's yield criterion, the distribution of stress in a fully plastic vessel is found. Based on the Tresca's criterion, if maximum shear stress gets to the yield level, Y , plastic deformation is practicable. Therefore, in an axi-symmetric problem if tangential stress, σ_θ , becomes greater than radial stress, σ_r , the yield criterion can be shown as,

$$\sigma_\theta(r) - \sigma_r(r) = Y(r) \tag{35}$$

Using equilibrium equation in Eq. (11), constitutional equations in Eqs. (1)–(4) and failure criterion in Eq. (35) one realizes that [17],

$$\sigma_r(r) = \frac{2r^m Y_o}{m} + Q_1 \tag{36}$$

$$\sigma_\theta(r) = \frac{(2+m)r^m Y_o}{m} + Q_1 \tag{37}$$

where Q_1 is depended on the boundary conditions. Plastic deformation is supposed to be incompressible, i.e., $\varepsilon_r^p(r) + \varepsilon_\theta^p(r) + \varepsilon_\phi^p(r) = 0$. Therefore, according to the stress-strain relationship the sum of strain components is,

$$\varepsilon_r^T(r) + 2\varepsilon_\theta^T(r) = \frac{(1-2\nu)}{E} (\sigma_r(r) + 2\sigma_\theta(r)) + 3\alpha(r).T(r) \tag{38}$$

Using Eqs. (7) and (8) one obtains,

$$\frac{du(r)}{dr} + \frac{u(r)}{r} = \frac{(1-2\nu)}{E} (\sigma_r(r) + 2\sigma_\theta(r)) + 3\alpha(r).T(r) \tag{39}$$

Substituting stress components from Eqs. (36) and (37), we have:

$$\frac{du(r)}{dr} + \frac{2u(r)}{r} = \left[\frac{2(1-2\nu)}{E_0} \cdot \frac{(3+m)Y_0}{m} \right] r^{m-n} + \frac{3Q_1(1-2\nu)}{E_0} r^{-n} + 3\alpha_0 T(r) r^L \quad (40)$$

By using of heat transfer equation provided in Eq. (17), the overall shape of the plastic displacement differential equation is,

$$\frac{du(r)}{dr} + \frac{2u(r)}{r} = \left[\frac{2(1-2\nu)}{E_0} \cdot \frac{(3+m)Y_0}{m} \right] r^{m-n} + \frac{3Q_1(1-2\nu)}{E_0} r^{-n} + 3\alpha_0 C_2 r^L + 3\alpha_0 C_1 r^{L-q-1} \quad (41)$$

Now we try to find the general solution of Eq. (41). The homogeneous form of Eq. (41) equation is,

$$\frac{du(r)}{dr} + \frac{2u(r)}{r} = 0 \quad (42)$$

To solve Eq. (42) we have,

$$\frac{du(r)}{u(r)} = -2 \frac{dr}{r} \quad (43)$$

$$u_p(r) = \frac{C_3}{r^2} \quad (44)$$

In which C_3 is a constant. A particular solution of Eq. (41) is,

$$u_p(r) = P_1 r^{L-q} + P_2 r^{L+1} + P_3 r^{m-n+1} + P_4 r^{1-n} \quad (45)$$

Substituting Eq. (45) in Eq. (41) provides:

$$\frac{du(r)}{dr} + \frac{2u(r)}{r} = P_1(L-q+2)r^{L-q-1} + P_2(L+3)r^L + P_3(m-n+3)r^{m-n} + P_4(3-n)r^{-n} \quad (46)$$

Then comparing Eqs. (46) and (41) yields,

$$P_1 = \frac{3\alpha_0 C_1}{L-q+2} \quad (47)$$

$$P_2 = \frac{3\alpha_0 C_2}{L+3} \quad (48)$$

$$P_3 = \frac{2(1-2\nu)(3+m)Y_0}{mE_0(m-n+3)} \quad (49)$$

$$P_4 = \frac{3Q_1(1-2\nu)}{E_0(3-n)} \quad (50)$$

Thus the fully plastic general solution of the displacement for a spherical vessel is,

$$u(r) = u_g(r) + u_p(r) = \frac{C_3}{r^2} + P_1 r^{L-q} + P_2 r^{L+1} + P_3 r^{m-n+1} + P_4 r^{1-n} \quad (51)$$

Once the displacement field is obtained, the plastic strain can be calculated as well. That is,

$$\varepsilon_\theta^p(r) = \frac{u(r)}{r} - \alpha(r) \cdot T(r) - \frac{[\sigma_\theta(r) - \nu(\sigma_r(r) - \sigma_\theta(r))]}{E(r)} \quad (52)$$

$$\varepsilon_r^p(r) = \frac{du(r)}{dr} - \alpha(r) \cdot T(r) - \frac{[\sigma_\theta(r) - 2\nu\sigma_\theta(r)]}{E(r)} \quad (53)$$

It should be mentioned that, in special case of $m = 0$, P_3 in Eq. (49) is undefined and this in turn causes Eqs. (51)–(53) to be undefined.

Therefore, when $m = 0$ Eqs. (51)–(53) are not applicable and the problem should be formulated separately from the beginning.

Using the Tresca's yield criterion (35), the equilibrium equation in (11) can be rewritten as,

$$\frac{d\sigma_r(r)}{dr} = \frac{2Y(r)}{r} \quad (54)$$

Consequently, the stress components are,

$$\sigma_r(r) = Q_1 + 2Y_0 \ln r \quad (55)$$

$$\sigma_\theta(r) = Q_1 + [1 + 2 \ln r] Y_0 \quad (56)$$

3. Discussions and results

In this work the position of elastic–plastic interface in a spherical inhomogeneous vessel obeying the elastic–perfectly plastic uni-axial stress-strain behavior and Tresca's failure criterion under different temperature and pressure distributions inside and outside the vessel are studied. Physical properties may differ only along the radial direction. Temperature distribution is in a steady state condition and the effect of temperature on material properties is negligible. Coefficients of elasticity, yield stress, thermal expansion and conductivity are power functions of radius. Throughout the thickness, Poisson's ratio is a constant independent of temperature. To locate the position of elastic–plastic border line, the related Navier equations of inhomogeneous material in elastic and plastic regions given in Eqs. (26) and (51) are solved simultaneously and unknown quantities in the interface line as well as the position of the interface line are obtained.

One of the main requirements of this analysis is to have at least a rough estimate of the plastic deformation onset radius. That is we must know whether plasticity begins from inside, outside or even from an intermediate radius. When internal pressure increases the stress in different radii of an axi-symmetric vessel grows up. In this condition, there is a radius wherein the left side of Eq. (35) grows up sooner to the key level of Y given in the right side of Eq. (35). This point is the plastic zone initiation point. Unlike the homogeneous materials in which plastic deformation begins from the inner surface of a spherical vessel, in general, for an inhomogeneous material, this onset point could be anywhere along the radius of the sphere. However, apart from the initiation of plastic zone, plastic zone growth pattern is also dissimilar in different material compositions. For example, in situations where plastic zone commences from an intermediate radius, it is likely that by increasing of internal pressure the separation line moves toward or out of the internal radii. As there are many conditions and parameters that can be assessed, here only a few typical examples are shown and studied.

In order to reduce the possibility of change in the yielding pattern during the transient heat transfer and to reduce the complexity of highly nonlinear problem, the assumption is that steady state thermal condition is shaped prior to the application of any mechanical pressure load and as a whole any types of path-dependent situation is not considered here.

It should be mentioned that in all cases, the boundary conditions of the steady state heat equation are of the Dirichlet or essential nature. Moreover, in all cases irrelevant to the inside

Table 1
The parameters used in the both examples.

E_0 (Pa)	Y_0 (Pa)	P_b (Pa)	b (m)	ν	f_2
2×10^{11}	4.3×10^8	0	1	0.3	0
α_0 ($^{\circ}\text{C}^{-1}$)	C_{11} ($^{\circ}\text{C}^{-1}$)	C_{12} ($^{\circ}\text{C}^{-1}$)	C_{21} ($^{\circ}\text{C}^{-1}$)	C_{22} ($^{\circ}\text{C}^{-1}$)	
1.2×10^{-6}	0	1	0	1	

Table 2
The parameters, plastic deformation starts from outside.

n	m	L	q	a (m)	P_a (Pa)
0.9	-2.8	-4	-4	0.4	3.5×10^9

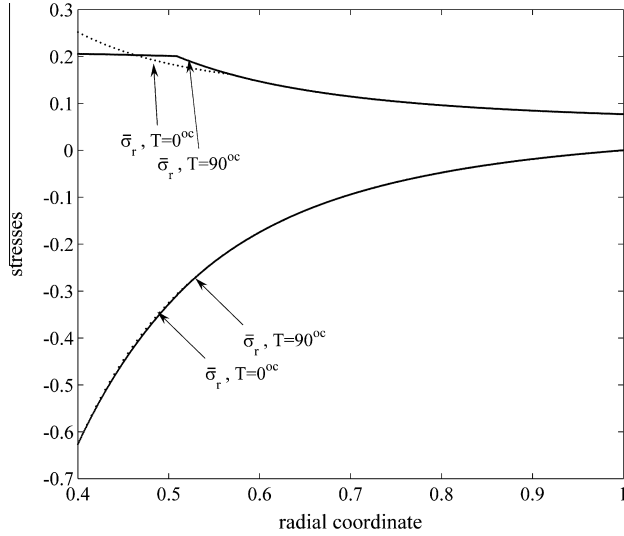


Fig. 2. Stress distribution in different temperatures, plastic zone begins from outside.

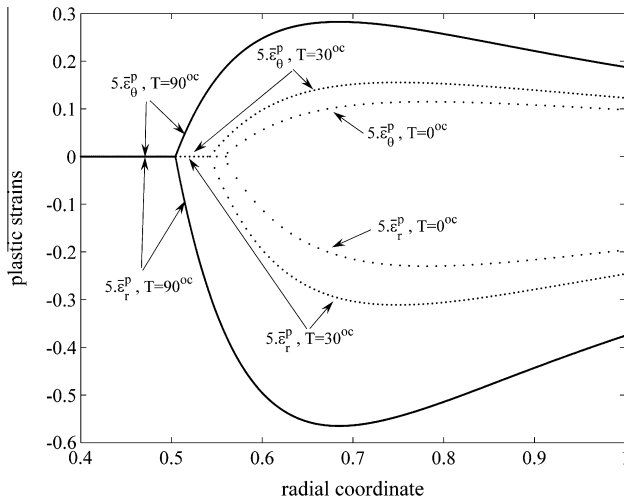


Fig. 3. Plastic strain distributions in different temperatures, plastic zone begins from outside.

temperature, the temperature in the outside is $T(b) = 0^\circ\text{C}$. A physical characteristic of the material are represented in Table 1 and is the same for both examples.

The radial variables as well as the stress and strain components in dimensionless form are proposed as,

$$\bar{r} = \frac{r}{b}; \quad \bar{\sigma}_\theta = \frac{\sigma_\theta}{Y_0 a^m}, \quad \bar{\sigma}_r = \frac{\sigma_r}{Y_0 a^m}, \quad \bar{\varepsilon}_r = \frac{\varepsilon_r \cdot E_0 \cdot b^n}{Y_0 a^m}, \quad \bar{\varepsilon}_\theta = \frac{\varepsilon_\theta \cdot E_0 \cdot b^n}{Y_0 a^m} \quad (57)$$

3.1. Case study 1

It is assumed that the rise of pressure triggers the plastic zone to start from the outer surface of a spherical vessel. To perform the

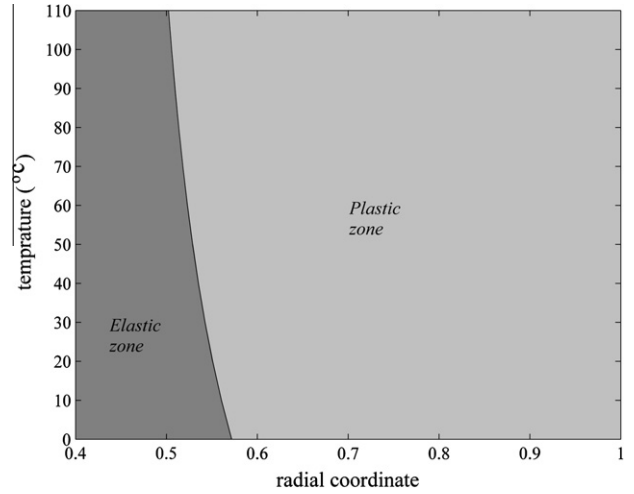


Fig. 4. The position of elastic and plastic zone interface line, plasticity begins from outside.

Table 3
The parameters, plastic zone starts from an intermediate radius.

n	m	L	q	a (m)	P_a (Pa)
-1.53	-4.2	1.2	1.2	0.3	3.123×10^{10}

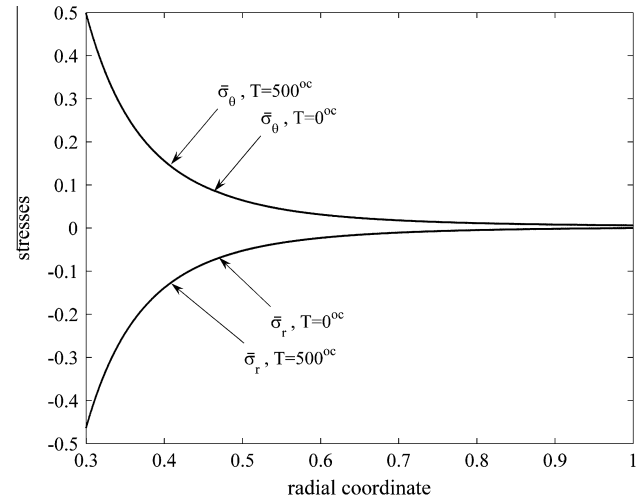


Fig. 5. Stress distribution in different temperatures, plastic zone begins from an intermediate radius.

analysis a sphere with the physical parameters given in Table 2 is considered. In Table 2 m, n, L and q are the exponents used in Eqs. (1)–(4), a is the internal radius of the vessel and P_a is the internal pressure.

To find the position of elasto-plastic interface line, some equations should be solved simultaneously. There are five unknown A_1, A_2, Q_1, C_3 and r_p . These unknowns are obtained by using of the following boundary conditions,

$$\sigma_r^e(a) = P_a; \quad \sigma_r^p(b) = P_b; \quad u^e(r^p) = u^p(r^p);$$

$$\sigma_r^e(r^p) = \sigma_r^p(r^p); \quad \sigma_\theta^e(r^p) = \sigma_\theta^p(r^p)$$

Based on these constraints the analysis has been performed. Using the results of the solution, the radial and tangential stresses are

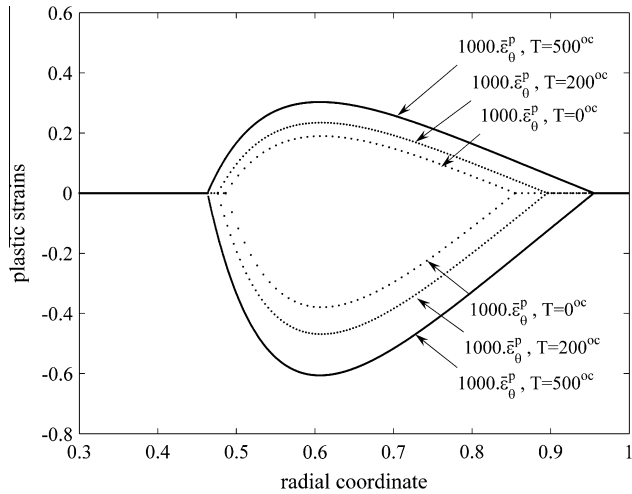


Fig. 6. Plastic strain distribution in different temperatures, plastic zone begins from an intermediate radius.

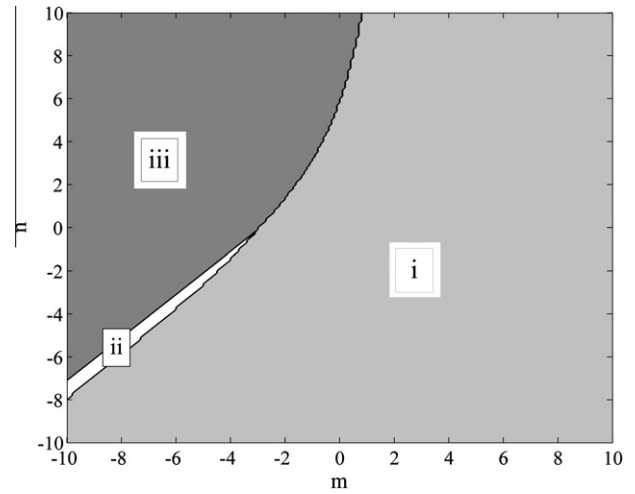


Fig. 8. The monograph of yielding pattern in different in-homogeneity m and n exponents.

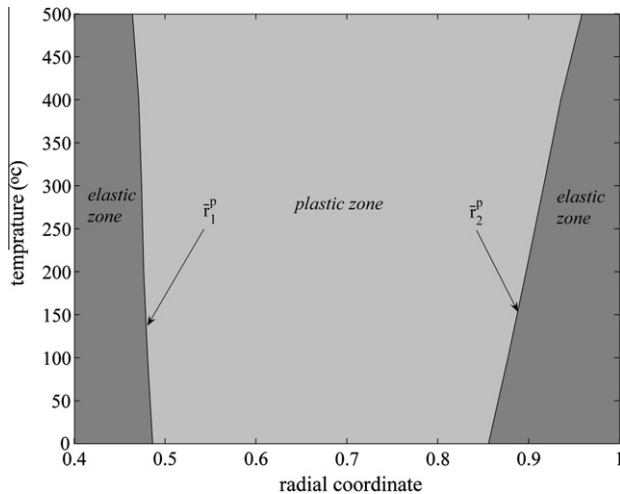


Fig. 7. The positions of elastic and plastic zone interface lines, plasticity begins from an intermediate radius.

plotted in Fig. 2. Likewise, the radial and tangential strains are given in Fig. 3 and the increase in plastic zone is shown in Fig. 4.

As can be seen in Fig. 4, the higher is the temperature inside the vessel, the bigger is the plastic zone area.

3.2. Case study 2

The second case shows a condition in which plastic zone starts from an intermediate radius between the inside and outside surfaces of a vessel with the parameters shown in Table 3. As usual m, n, L and q are the exponents used in Eqs. (1)–(4), a is the internal radius of the vessel and P_0 is the internal pressure.

In this case, there are eight equations and eight unknowns. For the interior elastic region ($a < r < r_1^p$) the unknowns are r_1^p, A_1 and A_2 . For the intermediate plastic zone ($r_1^p < r < r_2^p$) Q_1 and C_3 are the unknowns and for the exterior elastic zone ($r > r_2^p$) the unknowns are r_2^p, A_1 and A_2 . The boundary conditions are,

$$\begin{aligned} \sigma_r^e(a) &= P_a, & \sigma_r^e(b) &= P_b, & \sigma_r^e(r_1^p) &= \sigma_r^p(r_1^p), \\ \sigma_\theta^e(r_1^p) &= \sigma_\theta^p(r_1^p), & \sigma_r^e(r_2^p) &= \sigma_r^p(r_2^p), & \sigma_\theta^e(r_2^p) &= \sigma_\theta^p(r_2^p), \\ u^e(r_1^p) &= u^p(r_1^p), & u^e(r_2^p) &= u^p(r_2^p) \end{aligned}$$

In the above relationships r_1^p is the first elasto-plastic interface from the inside, r_2^p is the second elasto-plastic interface and the letters e and p indicate elastic and plastic regions, respectively. The solution for the stresses is given in Fig. 5 and strain curves are shown in Fig. 6. Fig. 7 shows that the increase of temperature shifts the borderlines existed between the elastic and plastic regions.

4. Yield pattern monograph

As seen in the former case studies, there may be different pattern for the commencement of yielding in a pressure vessel. That is the yielding may start from an internal radius, external radius or even somewhere in the bulk material of the vessel. The behavior is highly depended on the selection of exponents in the parameter distribution Eqs. (1)–(4). In order to shed light on this feature here a different graph is introduced. In the plane of this monograph, the color of each point denotes the yield pattern produced by the particular selection of the parameters shown in by ordinate and abscissa. That is the color of each point shows whether the yielding commences from inside, outside or from an intermediate radius. The boundary between each colored zone shows a marginal behavior similar to both adjacent patterns. For example, the boundary between (i) and (iii) zones designates a yield pattern in which yielding starts from inside and outside simultaneously.

The three different yield pattern zones in a wholly zero temperature condition are shown in Fig. 8. Zone (i) demonstrates a situation where plastic zone commences from inside. Zone (ii) points to the special arrangements of the material in-homogeneity exponents, which causes the plastic zone to show up in an intermediate radius. Zone (iii) belongs to the selections that results in the onset of plastic zone from the outer radii.

5. Conclusion

In a FGM spherical vessel, the effects of pressure and temperature upon the distribution of stress and yield pattern of are studied. To this ends, Tresca yield criterion and small deformation theory are assumed. Four characteristic factors including the elastic coefficient, yield stress, coefficient of thermal conductivity and coefficient of thermal expansion are considered as power functions of radius of vessel and independent of temperature. The Poisson's ratio is assumed to be a constant, independent of temperature. According to the results of this work, the structure of FG material,

the pressure and the steady state distribution of temperature may affect the spread and growth of plastic zone. Unlike the homogeneous materials in this generalized inhomogeneous case, the ever-growing area of plastic zone is not necessarily initiating inside. In this relation, several scenarios for the escalating and growth of plastic regions may be considered. That is plastic zone may start from inside, Outside, an intermediate radius or even may commences simultaneously from inside and outside. To entrap all categories inside a unique framework some monographs are represented which show how material parameters may influence the pattern of the yielding.

References

- [1] C.O. Horgan, A.M. Chan, *Journal of Elasticity* 55 (1999) 43–59.
- [2] N. Tutuncu, M. Ozturk, *Composites: Part B* 32 (2001) 683–686.
- [3] X.D. Zhang, D.Q. Liu, C.C. Ge, *Journal Functionally Graded Material* 25 (1994) 452–455.
- [4] S. Takezono, K. Tao, E. Imamura, M. Inove, *International Journal of Japan Society of Mechanical Engineers* 62 (1996) 474–481.
- [5] R.C. Wetherhold, S. Seelman, J.Z. Wang, *Computational Science Technology* 56 (1996) 099–1104.
- [6] R.W. Zimmerman, M.P. Lutz, *Journal of Thermal Stresses* 22 (1999) 77–188.
- [7] Y. Obata, K. Kanayamy, T. Ohji, N. Noda, *Proceeding of Thermal stresses* 99 (1999) 3–17.
- [8] H. Awaji, R. Sivakumar, *Journal of American Ceramic Society* 25 (2001) 059–1065.
- [9] J.N. Reddy, C.D. Chin, *Journal of Thermal Stresses* 21 (1998) 593–626.
- [10] J. Woo, S.A. Mequid, *International Journal of Solids and Structures* 38 (2001) 409–7421.
- [11] M. Jabbari, S. Sohrabpour, M.R. Eslami, *International Journal of Pressure Vessels and Piping* 79 (2002) 93–497.
- [12] R. Poultangari, M. Jabbari, M.R. Eslami, *International Journal of Pressure Vessels and Piping* 85 (2008) 95–305.
- [13] K.M. Liew, S. Kitipornchai, X.Z. Zhang, C.W. Lim, *International Journal of Solids and Structures* 40 (2003) 2355–2380.
- [14] M.R. Eslami, M.H. Babaei, R. Poultangari, thermal and mechanical stresses in a functionally graded thick sphere, *International Journal of pressure vessels and piping* 82 (2005) 522–527.
- [15] A.N. Eraslan, T. Akis, *International Journal of Pressure Vessels and Piping* 83 (2006) 635–644.
- [16] A. Bahtui, M.R. Eslami, *Mechanics Research Communications* 34 (2007) 1–18.
- [17] T. Akis, *Computational Materials Science* 46 (2009) 545–554.
- [18] Y. Obata, N. Noda, *Journal of Thermal Stresses* 17 (1994) 471–487.
- [19] Y. Ootao, Y. Tanigawa, T. Nakamura, *Composites: Part B* 30 (1999) 415–422.
- [20] H.S. Shen, *Composite Science and Technology* 62 (2002) 977–987.
- [21] R. Shahsiah, M.R. Eslami, *Journal of Thermal Stresses* 26 (2003) 277–294.
- [22] V.I. Alshits, H.O.K. Kirchner, *Proceeding of Royal Society of London* 457 (2001) 671–693.
- [23] A. Oral, G. Anals, *International Journal of Solids and Structures* 42 (2005) 5568–5588.